

Tactile-Based Motion Adjustment for the Nursing-Care Assistant Robot RIBA

Toshiharu Mukai, Shinya Hirano, Morio Yoshida, Hiromichi Nakashima, Shijie Guo and Yoshikazu Hayakawa

Abstract—In aging societies, there is a strong demand for robotics to tackle problems resulting from the aging population. Patient transfer, such as lifting and moving a bedridden patient from a bed to a wheelchair and back, is one of the most physically challenging tasks in nursing care. We have developed a prototype nursing-care assistant robot, RIBA, that can conduct patient transfer using human-type arms. The basic robot motion trajectories are created by interpolating several postures designated in advance. To accomplish more flexible and suitable motion, adjustment using sensor information is necessary, because the patient's posture and positions in contact with the robot may differ slightly in each trial. In this paper, we propose a motion adjustment method in patient lifting using tactile sensors mounted on the robot arms. The results of experiments using a lifesize dummy are also presented.

I. INTRODUCTION

With the advent of an aging society, the demand for human-interactive robots that can help on-site caregivers by playing a role in nursing humans, particularly the elderly, is increasing. For this purpose, many robots have been proposed, for example, robots for feeding people who are paralyzed [1], mental commitment robots dedicated to mental healing [2] and smart wheelchairs [3]. There are also wearing-type robots [4] that can support a caregiver's or patient's motion.

Tasks involving the transfer of patients, such as lifting and moving a bedridden patient from a bed to a wheelchair and back, are among the most physically challenging tasks in nursing care. Although patient-lifting devices have been developed and commercialized, they are not widely used in nursing-care facilities in Japan. According to [5], the proportion of caregivers in Japanese nursing-care facilities always or sometimes using portable patient lifts is only 14.8%. The reasons for this include the long time required for their use, the difficulty of attaching slings, the risk of dropping a patient, and the mental and physical discomfort of the patient.

With this background, robotics is required to help with patient-transferring tasks. Daihen Corporation has developed

T. Mukai, S. Hirano, M. Yoshida and H. Nakashima are with RIKEN RTC, 2271-130, Anagahora, Shimoshidami, Moriyama-ku, Nagoya 463-0003, Japan {tosh, hirano, yoshida, nakas}@nagoya.riken.jp

S. Guo is with SR Laboratory, Tokai Rubber Industries, 1, Higashi 3-chome, Komaki, Aichi 485-8550, Japan shiketsu.kaku@tri.tokai.co.jp

Y. Hayakawa is with RIKEN RTC and Nagoya University, Furo-cho, Chikusa-ku, Nagoya 464-8601, Japan hayakawa@nuem.nagoya-u.ac.jp



Fig. 1. RIBA lifting a human in its arms.

a patient-transfer apparatus named C-Pam [6] that can transfer a patient between a bed and a stretcher. It consists of a flat board covered with motorized endless belts, and gently crawls under the patient who is lying on the bed. Panasonic developed the Transfer Assist Robot [7], which has flat board-type arms with motorized endless belts, and can transfer a patient from a bed to an almost flat wheelchair with a reclining function. However, these robots cannot transfer a patient to widely used types of wheelchair without reclining function. The long time taken to use these devices is another drawback. Another approach to assisting with transfer tasks by robotics is the use of wearing-type robots [4]. A robot of this type is worn by the caregiver and assists his or her motion. In nursing-care facilities, however, caregivers have to perform many other tasks in addition to patient transfer, and wearing such a robot may interfere with these tasks.

We consider that robots for performing patient-transfer tasks between a bed and a wheelchair are needed in nursing-care facilities and hospitals. To this end, we have developed a prototype nursing-care assistant robot, RIBA [8] (Fig. 1). RIBA can transfer a human between a bed and a wheelchair, using human-type arms. As the target patients for the moment, we consider those who can stay still during transfer, and are without skin or joint troubles. RIBA is equipped with tactile sensors on a wide area of its arms. These tactile sensors can be used for giving instructions to the robot and for sensor feedback to adjust patient-transfer motions.

In this paper, we propose a method of adjusting patient-lifting motions by detecting the state of contact between the robot and the lifted person using tactile sensors, to enable comfortable lifting. The sensors can detect two-dimensional pressure patterns on its arms. Depending on the sensor output, the motion trajectories are modified for the given

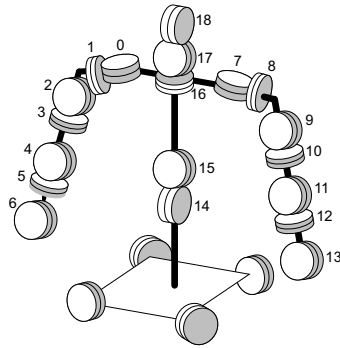
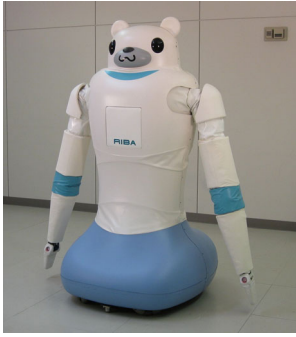


Fig. 2. RIBA (Robot for Interactive Body Assistance) and its joint configuration.

TABLE I
BASIC SPECIFICATIONS OF RIBA.

Dimensions	Width	750 mm (when arms are folded)	
	Depth	840 mm	
	Height	1,400 mm	
Weight inc. batteries		180 kg	
D.O.F.	Head	3 (only 1 in current use)	
	Arm	7 each	
	Waist	2	
	Cart	3 (with 4 motored wheels)	
Base movement		Omnidirectional with omnidirectional wheels	
Actuator type		DC motor	
Payload		63 kg (tested value)	
Operation time		2 hour in standard use	
Power		NiMH batteries	
Sensors	Vision	2 cameras	
	Audio	2 microphones	
	Tactile	Upper arm	128 pts. each
		Forearm	94 pts. each
		Hand	4 pts. each
Shoulder pad	8 pts. each		

situation. Some robots with tactile sensors on a wide area of their surfaces have already been proposed. However, the sensors were used for human-robot communication [9] or contact state identification [10]. The robot in [11] lifted up a box using its arms, but tactile sensors were used only for detecting the size and position of the box and the contact state. We propose motion trajectory adjustment based on tactile sensor output.

II. ROBOT SPECIFICATIONS

We explain RIBA's specifications briefly, mainly focusing on the features that are relevant to the proposed tactile-based motion adjustment. For more detailed information, please refer to [8].

RIBA and its joint configuration are shown in Fig. 2, and its basic specifications are summarized in Table I. To provide a large power with compact motors, most joints in RIBA have high gear ratios (> 1000). As a result, the joints in RIBA have no backdrivability. We apply position control to these joints, and use sensor feedback when a soft response to physical contact is needed.

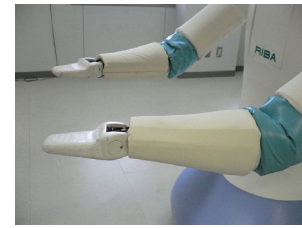


Fig. 3. Forearms, the shape of which fits the human back.



(a) Without cover (b) With cover

Fig. 4. Tactile sensors on the upper arm.

To ensure safety in the case of unexpected contact, as well as the stability and comfort of the lifted person, the entire body of RIBA including its joints is covered with soft materials such as polyurethane foam and a silicone elastomer. During lifting, as shown in Fig. 1, a large proportion of the lifted person's weight is supported by the forearms. To ensure comfortable contact for the lifted person, the forearms have a slightly concave surface that fits the human back, as shown in Fig. 3.

For tactile sensors, we developed a flexible tactile sheet with 8×8 semiconductor pressure sensors and a readout circuit embedded in an elastic material [12]. This type of tactile sensor is mounted on the upper arms (Fig. 4) and forearms. Two tactile sheets were used to cover the front and back of each upper arm or forearm, so as to cover the whole circumference. The tactile sheets on the forearm are cut into a comblike shape with some of the teeth of the comblike shape cut off to fit the complex shape of the forearm. The numbers of sensing-elements on each upper arm and forearm are 128 and 94, respectively. The measurement range is wider than 0 - 90 kPa and the measurement resolution of each sensing-element is more than 5 bit. This enables the detection of soft touch by a human finger and the weight of a human on the arms.

The basic trajectories of motion are created by interpolating several postures designated in advance. Each type of motion is selected using voice commands such as 'Lift up from the bed'. Motions that involve physical interaction with a human, however, need adjustment to the actual situation. Tactile sensors can detect contact states that are essential in the adjustment. Additional vision sensors may be helpful, though they cannot directly detect contact in many cases because of occlusion. As the first step of research, we use only tactile sensors for adjustment.

RIBA can operate as a stand-alone robot since all its processors and batteries are installed internally. The main PC (CPU: Intel CoreDuo, 2 GHz) and more than 20 local processing boards (CPU: Microchip dsPIC33F) to control

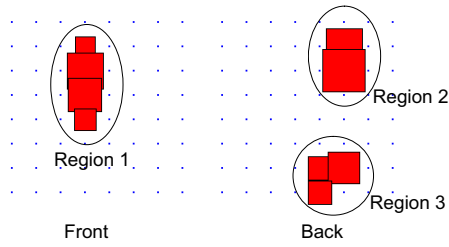


Fig. 5. Regions are detected from the tactile sensor output and features are calculated for each region.

the sensors or motors constitute the distributed information-processing network in RIBA. This distributed network contributes to reducing the computational load of the main PC, decreasing the number of cables in RIBA, and reducing the sensor noise by shortening the analog transmission length. The output of a tactile sensor is captured by its local controller using an A/D converter. Then two-dimensional pattern information is processed locally and only the extracted features are sent to the main PC via the network. The control loop periods of the tactile sensor controllers, the motor controllers, and the main PC are 4 ms, 1 ms, and 10 ms, respectively.

RIBA has succeeded in lifting a human from a bed, placing a human on a bed, lifting a human from a wheelchair, putting a human down on a wheelchair, and moving with a human in its arms. The current maximum weight of the lifted person is 63 kg.

III. TACTILE PATTERN PROCESSING

The tactile sensors on RIBA provide two-dimensional pressure pattern information on the curved surfaces of the upper arms and forearms. Their output is used in sensor feedback to enable comfortable lifting. It is also used to detect the operator's commands through touch, which was proposed and named as 'tactile guidance' in [8]. In short, this is a method to intuitively give the operator's instruction by touching the part concerning the motion, as a teacher instructs the motion of a student through touch and directly guides the student's motion when teaching sport or dance.

Pattern processing is applied to the two-dimensional pressure information to distinguish contact with the lifted person from that with the operator. For this purpose, regions consisting of neighboring active elements are detected first (Fig. 5). Then for each region, feature values such as the area, the center of pressure, the sum of pressures, and the maximum pressure are calculated. The position of the center of pressure and the sum of pressures are used to determine whether or not pressure at a certain region is caused by the weight of the lifted person, according to the predicted touching location and force for lifting.

Basically, regions are detected and feature values are calculated using methods similar to image processing (for example, see [13]). However, we cannot simply apply image-processing methods because the robot surfaces are not planar.

First, the surface may be circular, which causes difficulty when calculating geometrical features such as the center of

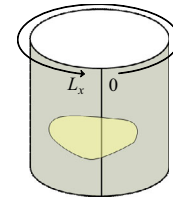


Fig. 6. Coordinates on a circular surface.

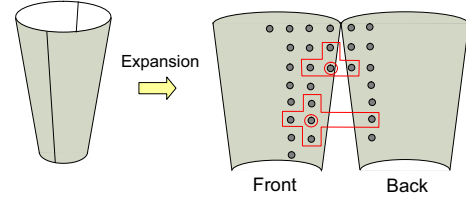


Fig. 7. Alternative definitions of 4-neighbor elements on expanded planes.

pressure. Let us assume that the x -direction is circular and its coordinates are from 0 to L_x . Let (x, y) denote a sensing-element position and $p(x, y)$ its pressure output. Then if a region is on a line of discontinuity, as shown in Fig. 6, and we simply calculate the x -coordinate of the center of pressure as

$$x_{\text{cop}} = \frac{1}{S} \sum_{(x,y) \in A} xp(x, y), \quad (1)$$

where $S = \sum_{(x,y) \in A} p(x, y)$ and A is the region under consideration, the resultant x_{cop} is about $L_x/2$, which is incorrect. To solve this problem, we define new coordinates,

$$\tilde{x} = x + nL_x, \quad (2)$$

where n is an appropriate integer to make the coordinates continuous on the region. Geometrical features are calculated using this \tilde{x} -coordinate, and to obtain the final results, the geometrical values are mapped onto $[0, L_x)$.

Surfaces that cannot be expanded into a rectangular plane cause another problem. We use 4-neighbor connectivity on the expanded planes to determine regions with neighboring active elements. However, if the expanded planes are not rectangular, we cannot determine the 4-neighbor elements in the normal sense. An example of this is given in Fig. 7, where some elements are cut off, and separate elements on the expanded planes are made neighbors on the original curved surface. We use alternative definitions of 4-neighbor elements as shown in Fig. 7, where the elements under consideration are circled and their neighbors are enclosed by lines.

IV. TACTILE-BASED MOTION ADJUSTMENT

A. Outline of Motion Adjustment

The basic motions of RIBA are created by interpolating several designated postures. In patient-transfer motions such as lifting up from a bed, the postures are determined with reference to human patient-transfer motions. Interpolation is conducted in joint angle space.

The motions thus made, however, need adjustment. We here consider the motion of lifting up shown in Fig. 8 and

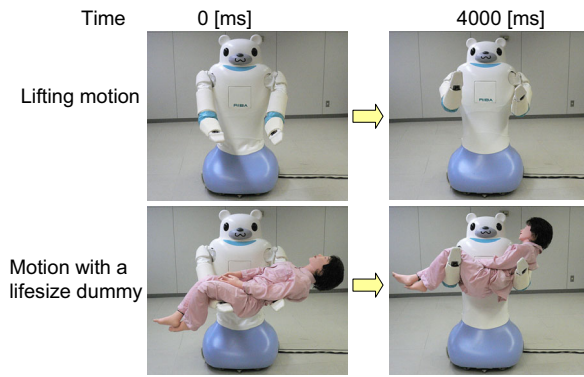


Fig. 8. Lifting motion with and without a lifesize dummy.

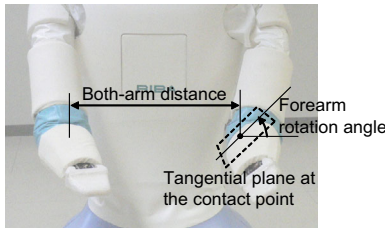


Fig. 9. Both-arm distance and forearm rotation angle.

in the accompanying video. This motion is usually applied to a person on a bed, but we did not use a bed in the following experiments to illustrate the motion more clearly. According to comments from the lifted persons in the lifting experiments in [8], the following requirements should be satisfied to ensure comfort during lifting (Fig. 9).

- Keeping the distance between both arms at a suitable value so that the body of the lifted person can fit between the arms.
- Matching the rotation angle of the forearm to the back of the lifted person so that the concave surface of the forearm fits the back.

Although these requirements should be met, the overall posture of the robot is also important. This is because, in the lifting in Fig. 1, not only the forearms but also the upper arms and the chest are in contact with the lifted person. Therefore, we meet the above requirements while maintaining the originally designated postures and their interpolations as far as possible. We refer to the distance in a) as the ‘both-arm distance’, and the forearm and its rotation angle in b) as the ‘back-supporting forearm’ and ‘back-supporting angle’, respectively, in this paper. The ideal values of the both-arm distance and back-supporting angle are determined based on the trial and error with the opinions from the lifted person.

We adopt two-stage motion adjustment as shown in Fig. 10. These stages are conceptual and actual adjustment in both stages is conducted simultaneously. In the first stage, a motion devised by interpolation is fed to a converter outputting a motion that satisfies as far as possible the desired values of both-arm distance and back-supporting angle given as constraints. The positions of contact between the forearms and the lifted person detected by tactile sensors is also fed to

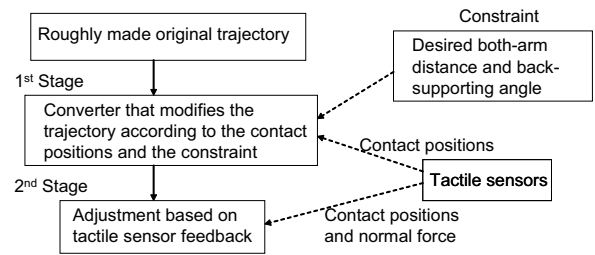


Fig. 10. Outline of trajectory adjustment using tactile sensor.

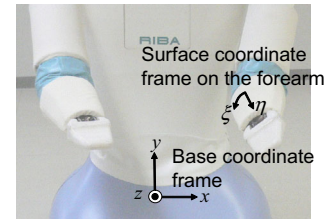


Fig. 11. Coordinate frames on RIBA.

the converter, because the motion outputted by this converter depends on these positions.

The output from the converter in the first stage may not be optimal for the actual situation because the desired values given as constraints may not be suitable owing to the incorrect estimation of these values or the variation of the lifted person’s posture and positions of contact in each trial. In addition, it is desirable to use a single patient-transfer motion for people with similar physiques. For these reasons, in the second stage, sensor feedback is applied to adjust the both-arm distance and back-supporting angle to suitable values for the actual situation.

We adopt two coordinate systems (Fig. 11). One is relative to the frame fixed on the robot’s cart and is referred to as the base coordinates, $\mathbf{x} = [x, y, z]^T \in \mathcal{R}^3$, where T represents the transpose of the vector. We do not consider the cart motion in this paper; thus, the base coordinates are the same as the world coordinates. The other is the surface coordinates, $\boldsymbol{\xi} = [\xi, \eta]^T \in \mathcal{R}^2$, on the robot’s curved surfaces. They are used to specify positions on the robot’s surfaces and they are relative to the link to which the surface belongs.

B. First Stage: Trajectory Modification Based on the Contact Positions

To modify the given trajectory to one that satisfies the constraints on the both-arm distance and back-supporting angle, we construct a converter that receives the current joint angles of the original trajectory, the constraint and the contact positions as the input and outputs the modified joint angles. The converter uses only time-local information so that the original trajectory and the constraint can be changed online.

The both-arm distance depends on the positions of contact between both arms and the lifted person. In the current setup of RIBA, however, the leg-side contact position cannot be detected stably because legs may rest against insensitive regions on the arm. We use the center of pressure on the

back-supporting forearm as the contact position on this arm. The contact position on the other forearm is determined under the assumption that the lifted person (or a lifesize dummy) is parallel to RIBA's body in the current way of lifting.

Let \mathbf{x}^L and \mathbf{x}^R respectively denote the left and right forearm contact points expressed in base coordinates. Let ξ^L and ξ^R be their corresponding surface coordinates. We also use the combination of coordinates as

$$\mathbf{X} = [\mathbf{x}^{L:T}, \mathbf{x}^{R:T}]^T \in \mathcal{R}^6, \quad \Xi = [\xi^{L:T}, \xi^{R:T}]^T \in \mathcal{R}^4.$$

Let $\theta \in \mathcal{R}^N$ be the joint angle vector necessary to determine \mathbf{X} corresponding to Ξ , where N is the relevant number of degrees of freedom. In RIBA's case, all joints except those of the wrists and head are used to determine \mathbf{X} , thus $N = 14$. We define the forward kinematic function from θ to \mathbf{X} corresponding to Ξ as

$$\mathbf{X} = T(\theta; \Xi). \quad (3)$$

Let $d = d(\mathbf{X})$ denote the both-arm distance and d_d its desired value. We define the converter in the first stage with input θ_{in} and output θ_{out} in terms of sampling time t as

$$\mathbf{X}_{\text{in}}(t) = T(\theta_{\text{in}}(t); \Xi(t)) \quad (4)$$

$$\mathbf{X}_{\text{out}}(t) = \mathbf{X}_{\text{in}}(t) + \mathbf{X}_{\text{mod}}(t) \quad (5)$$

$$\theta_{\text{out}}(t) = T^{-1}(\mathbf{X}_{\text{out}}(t); \Xi(t), \theta_{\text{init}}(t)). \quad (6)$$

Here, $\mathbf{X}_{\text{mod}}(t)$ is the modification vector used to satisfy the both-arm distance constraint and $\theta = T^{-1}(\mathbf{X}; \Xi, \theta_{\text{init}})$ is the inverse function of $\mathbf{X} = T(\theta; \Xi)$. The inverse function outputs the nearest value to θ_{init} in the least-square senses from the multiple possible solutions. The modification vector is updated every sampling time t by

$$\mathbf{X}_{\text{mod}}(t) = \mathbf{X}_{\text{mod}}(t-1) + \epsilon_1 \left(\frac{\partial d(t-1)}{\partial \mathbf{X}} \right)^\dagger (d_d(t) - d(t-1)), \quad (7)$$

where $\mathbf{X}_{\text{mod}}(0) = \mathbf{0}$, \dagger represents the generalized inverse and $d(t-1)$ is the abbreviation of $d(\mathbf{X}_{\text{out}}(t-1))$. This calculation rule is extracted by solving $\Delta \mathbf{X}_{\text{mod}}$ in

$$\begin{aligned} d_d(t) &= d(\mathbf{X}_{\text{in}}(t-1) + \mathbf{X}_{\text{mod}}(t-1) + \Delta \mathbf{X}_{\text{mod}}) \\ &\approx d(t-1) + \frac{\partial d(t-1)}{\partial \mathbf{X}} \Delta \mathbf{X}_{\text{mod}}. \end{aligned} \quad (8)$$

To gradually change the trajectory, we restrict the change using a coefficient ϵ_1 ($0 < \epsilon_1 \leq 1$). The inverse function in (6) is computationally solved by iterative calculations with the initial value θ_{init} . This value should be close to the resultant output because the number of possible iterations is limited in real-time motion adjustment. The initial value, corresponding to the predicted converter output, is calculated as

$$\theta_{\text{init}}(t) = \theta_{\text{in}}(t) + \rho(\theta_{\text{out}}(t-1) - \theta_{\text{in}}(t-1)), \quad (9)$$

where $\theta_{\text{init}}(0) = \theta_{\text{in}}(0)$ and ρ ($0 < \rho \leq 1$) is a coefficient used to maintain the output trajectory close to the input trajectory, thus preserving the original posture as far as possible. In this paper, we use the following simple definition of d :

$$d(\mathbf{X}) = |\mathbf{x}^L - \mathbf{x}^R|, \quad (10)$$

where x^L and x^R are the x -elements of \mathbf{x}^L and \mathbf{x}^R , respectively, and the x -axis is along the sideways direction of RIBA. In this definition and under the condition $x^L \geq x^R$, which is always true in the lifting motion,

$$\left(\frac{\partial d(t-1)}{\partial \mathbf{X}} \right)^\dagger = \frac{1}{2}[-1, 0, 0, 1, 0, 0]^T. \quad (11)$$

The adjustment of the back-supporting forearm is as follows. We assume that the lifted person is parallel to RIBA's body as described above, so that the angles in the xy -plane should be considered. Thus, we consider the intersection of the xy -plane and the plane tangential to the back-supporting forearm at the contact point. The angle of the line made by this intersection relative to the x -axis is the back-supporting angle. Let $a = a(\theta)$ denote the back-supporting angle and a_d its desired value.

To satisfy requirement b), we do not solve the inverse kinematic problem here but directly change the rotation angle of the forearm under the assumption that the forearm is almost perpendicular to the xy -plane, in order to preserve the original angles of the other joints. Let θ_{i_f} be the joint angle of the back-supporting forearm. In RIBA's case, if the head of the lifted person faces the positive direction of x , then $i_f = 12$. We replace $\theta_{\text{in};i_f}$ in (4) by

$$\theta_a(t) = \theta_a(t-1) + \epsilon_2(a_d(t) - a(t-1)) \quad (12)$$

$$\theta_{\text{in};i_f}^{\text{new}}(t) = \theta_{\text{in};i_f}^{\text{original}}(t) + \theta_a(t), \quad (13)$$

where $\theta_a(0) = 0$, $a(t-1)$ is the abbreviation of $a(\theta(t-1))$ and ϵ_2 ($0 < \epsilon_2 \leq 1$) is a coefficient to enable gradual trajectory change. Keeping ϵ_2 small also suppresses problems caused by the deviation from the perpendicular assumption.

C. Second Stage: Sensor Feedback Control of the Both-Arm Distance and Back-Supporting Angle

To deal with the difference between the ideal and actual situations, the ideal trajectory obtained in the first stage is adjusted by sensor feedback control using tactile sensors.

To adjust the both-arm distance, impedance control is used. Tactile sensors on RIBA can detect forces normal to its surfaces. If the lifted person is confined into a smaller space than the appropriate one between both arms during lifting, the pressing force causes a tactile sensor output. It should also be noted that the weight of the lifted person during appropriate lifting also invokes a tactile sensor output.

To detect only the deviation from the ideal lifting, we use the tactile sensor output recorded during ideal lifting in advance as a reference. The ideal sensor output differs according to the physique of the lifted person, so we record it for each person. Let $F(t)$ be the detected normal force at t obtained by summing the sensor outputs of the left and right forearms, and $F_{\text{rec}}(t)$ be its corresponding ideal value recorded in advance. If the force is excessive, the both-arm distance should be increased and if it is too small, the distance should be shortened. To accomplish this, $d_d(t)$ in (7) is replaced by

$$M_d \ddot{d}_{\text{imp}}(t) + D_d \dot{d}_{\text{imp}}(t) + K_d d_{\text{imp}}(t) = F(t) - F_{\text{rec}}(t) \quad (14)$$

$$d_d^{\text{new}}(t) = d_d^{\text{original}}(t) + d_{\text{imp}}(t), \quad (15)$$

where M_d, D_d, K_d are virtual inertia, viscosity, and stiffness, respectively. The impedance calculation using (14) is actually performed at discrete sampling times t , although it is shown here as a continuous function of time for a concise description.

To adjust the back-supporting angle in response to the actual contact, we use the position of the center of pressure on the contact region. Let $\xi^f(t)$ be the ξ -element in surface coordinates of the actual contact position on the back-supporting forearm at t and $\xi_d^f(t)$ be its ideal value. We aim to rotate the forearm so that the contact position comes at the center of the concave surface with respect to the ξ -direction (i.e., the circumference direction), which is expressed by $\xi_d(t) \equiv 0$. The equation used for back-supporting angle adjustment (13) is replaced by

$$M_\theta \ddot{\theta}_p(t) + D_\theta \dot{\theta}_p(t) + K_\theta \theta_p(t) = C_\theta (\xi_d^f(t) - \xi^f(t)) \quad (16)$$

$$\theta_{\text{in};i_f}^{\text{new}}(t) = \theta_{\text{in};i_f}^{\text{original}}(t) + \theta_a(t) + \theta_p(t), \quad (17)$$

where $M_\theta, D_\theta, K_\theta$ are virtual inertia, viscosity, and stiffness, respectively, and C_θ is a constant used to convert the dimension from length to torque. Here again, the impedance calculation is actually performed at discrete sampling time t , although it is shown as a continuous function of time for a concise description.

V. EXPERIMENTS

A. Experiments Using a Lifesize Dummy

The goal of the proposed method is its application to the motion of lifting a human. In experiments reported in this paper, however, we used a lifesize dummy, because the experimental motions may be uncomfortable or dangerous and should not be applied to humans from the viewpoint of research ethics. Regarding repeatability and objectivity, experiments with the dummy are also preferable. The height of the dummy is 148 cm and its weight is 18.5 kg. Although the weight is less than that of an adult human, the basic properties of our proposed method can be tested with the dummy. In the experiments, the desired both-arm distance and back-supporting angle were set to the constant values of

$$d_d(t) \equiv 400 \text{ [mm]}, \quad a_d(t) \equiv 0.7 \text{ [rad]}. \quad (18)$$

The used constant values are summarized in Table II.

B. Converting Trajectories in the First Stage

To confirm the effect of the converter in the first stage, we recorded the original and output trajectories. The contact position was set at 120 mm from the elbow joint. In this experiment, we set the contact position directly without using the sensor output in order to observe only the effect of touching positions. The both-arm distance, the back-supporting angle and the joint angles of the left arm from J7 to J12 are shown in Fig. 12. The converter was activated at 1000 ms to observe its effect.

TABLE II
CONSTANTS IN THE EXPERIMENTS.

Symbol	Value	Unit
ϵ_1	0.2	—
ϵ_2	0.3	—
ρ	0.99	—
M_d	200	kg
D_d	1500	kg/s
K_d	1500	kg/s ²
C_θ	1	kg·m/s ²
M_θ	53.3	kg·m ²
D_θ	266	kg·m ² /s
K_θ	133	kg·m ² /s ²

The results in (a) of Fig. 12 show that the converter outputs trajectories that realize the ideal both-arm distance and back-supporting angle. The original joint angle trajectories in (b) were changed to those in (c) by the converter, to satisfy the constraints.

C. Both-Arm Distance Adjustment in the Second Stage

The adjustment of both-arm distance in the second stage was tested using the dummy. RIBA took the posture of lifting and we intentionally squeezed the dummy into the space between RIBA's both arms, which caused excessive normal force on the tactile sensors. We recorded the both-arm distance and the force obtained from the tactile sensor output.

The results when both-arm distance adjustment was turned on and off several times are shown in Fig. 13. The pre-recorded reference force F_{rec} was 85 N in this posture. The both-arm distance, as the input of position control, increased to reduce the excessive force compared with the reference force. The change in both-arm distance depends on the impedance constants, and here we set them to cause a small change because a large change may have caused the dummy to be dropped.

A scene capturing both-arm distance adjustment is included in the accompanying video.

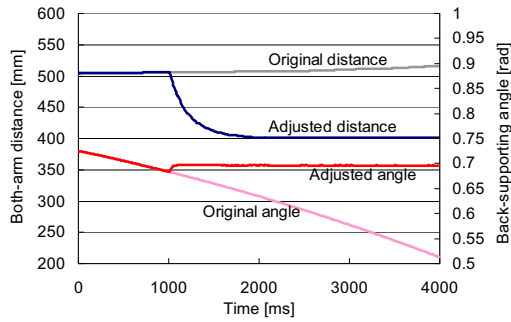
D. Back-Supporting Angle Adjustment in the Second Stage

The adjustment of the back-supporting angle was also tested using the dummy. We recorded the back-supporting angle, as the input of position control, and the ξ -coordinate of the center of pressure when RIBA took the posture of lifting and back-supporting angle adjustment was turned on and off several times. The target ξ -coordinate was 0 mm. The results in Fig. 14 show that the proposed method succeeded in controlling the back-supporting angle.

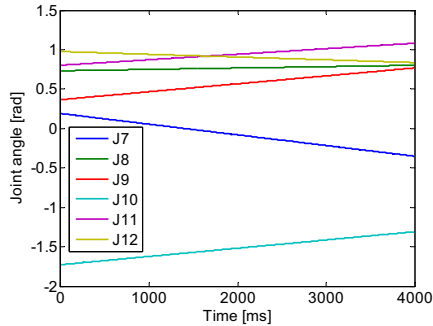
A scene capturing back-supporting angle adjustment is also included in the accompanying video.

VI. CONCLUSION

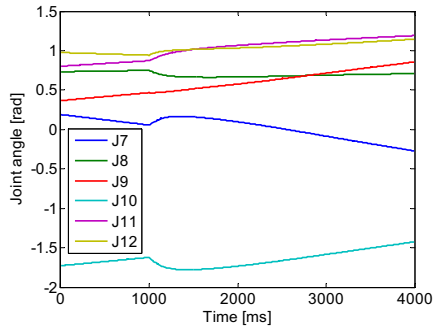
We proposed a tactile-based motion adjustment method for the nursing-care assistant robot RIBA. The both-arm distance and back-supporting angle of a patient-lifting motion was considered. We adopted a two-stage method, where a given original trajectory is modified to the ideal trajectory on the



(a) Both-arm distance and back-supporting angle with and without adjustment



(b) Original trajectories of J7 to J12



(c) Adjusted trajectories of J7 to J12

Fig. 12. Trajectories of the original and converted motions. The contact point was set at 120 mm and the converter was activated at 1000 ms.

basis of the detected contact position in the first stage, and the ideal trajectory is adjusted using tactile sensor feedback depending on the actual situation in the second stage. This method was developed for the lifting motions of RIBA but can also be used with slight modification for other motions of RIBA and for those of other human-interactive robots.

The proposed method was confirmed to work in experiments using a lifesize dummy. The constants were set tentatively for the experiments with the dummy and should be optimized for humans in future experiments.

REFERENCES

[1] My Spoon WEB page: <http://www.secom.co.jp/english/myspoon/>
 [2] K. Wada, T. Shibata, T. Saito, and K. Tanie, "Psychological and Social Effects in Long-Term Experiment of Robot Assisted Activity to Elderly People at a Health Service Facility for the Aged," in *Proc. IEEE/RSJ International Conference on Intelligent Robots and Systems (IROS)*, pp.3068–3073, 2004.

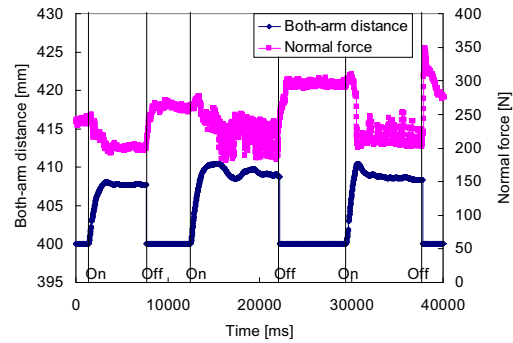


Fig. 13. Trajectories when both-arm distance adjustment was turned on and off.

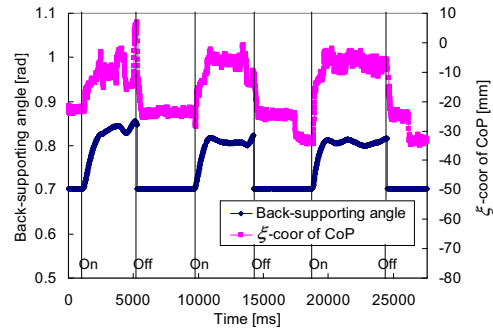


Fig. 14. Trajectories when back-supporting angle adjustment was turned on and off.

[3] C. Mandel, T. Lüth, T. Laue, T. Röfer, A. Gräser, and B. Krieg-Brückner, "Navigating a Smart Wheelchair with a Brain-Computer Interface Interpreting Steady-State Visual Evoked Potentials," in *Proc. IEEE/RSJ International Conference on Intelligent Robots and Systems (IROS)*, pp.1118–1125, 2009.
 [4] T. Hayashi, H. Kawamoto, and Y. Sankai, "Control Method of Robot Suit HAL Working as Operator's Muscle Using Biological and Dynamical Information," in *Proc. IEEE/RSJ International Conference on Intelligent Robots and Systems (IROS)*, pp.3455–3460, 2005.
 [5] K. Iwakiri, M. Takahashi, M. Sotoyama, M. Hirata, and N. Hisanaga, "Usage Survey of Care Equipment in Care Service Facilities for the Elderly," *J. Occupational Health*, Vol.49, pp.12–20, 2007 (in Japanese).
 [6] H. Wang and F. Kasagami, "A Patient Transfer Apparatus Between Bed and Stretcher," *IEEE Trans. on Systems, Man, and Cybernetics-Part B (Cybernetics)*, Vol.38, No.1, pp.60–67, 2008.
 [7] Y. Kume and H. Kawakami, "Development of Power-Motion Assist Technology for Transfer Assist Robot," *Matsushita Technical Journal*, Vol.54, No.2, pp.50–52, 2008 (in Japanese).
 [8] T. Mukai, S. Hirano, H. Nakashima, Y. Kato, Y. Sakaida, S. Guo, and S. Hosoe, "Development of a Nursing-Care Assistant Robot RIBA That Can Lift a Human in Its Arms," in *Proc. IEEE/RSJ International Conference on Intelligent Robots and Systems (IROS)*, pp.5996–6001, 2010.
 [9] N. Mitsunaga, T. Miyashita, H. Ishiguro, K. Kogure, and N. Hagita, "Robovie-IV: A Communication Robot Interacting with People Daily in an Office," in *Proc. IEEE/RSJ International Conference on Intelligent Robots and Systems (IROS)*, pp.5066–5072, 2006.
 [10] H. Iwata and S. Sugano, "Human-Robot-Contact-State Identification Based on Tactile Recognition," *IEEE Trans. on Industrial Electronics*, Vol.52, No.6, pp.1468–1477, 2005.
 [11] Y. Ohmura and Y. Kuniyoshi, "Humanoid Robot which can Lift a 30kg Box by Whole Body Contact and Tactile Feedback," in *Proc. IEEE/RSJ International Conference on Intelligent Robots and Systems (IROS)*, pp.1136–1141, 2007.
 [12] T. Mukai and Y. Kato, "1 ms Soft Areal Tactile Giving Robots Soft Response," *J. Robotics and Mechatronics*, Vol.20, No.3, pp.473–480, 2008.
 [13] OpenCV Wiki: <http://opencv.willowgarage.com/wiki/>